

## Geometrical Characterization and Effect of Temperature on Graphene Nanoparticles Conductive Ink

Adzni Md. Saad<sup>1,2</sup>, Mohd Azli Salim<sup>1,2,3\*</sup>, Murni Ali<sup>4</sup>, Feng Dai<sup>5</sup>, Siti Amirah Abdullah<sup>1</sup> and Faizil Wasbari<sup>1</sup>

<sup>1</sup>Fakulti Kejuruteraan Mekanikal, Universiti Teknikal Malaysia Melaka, Hang Tuah Jaya, 76100 Durian Tunggal, Melaka, Malaysia

<sup>2</sup>Intelligent Engineering Technology Services Sdn. Bhd., No.1, Jalan TU43, Taman Tasik Utama, 76450 Ayer Keroh, Melaka, Malaysia

<sup>3</sup>Advanced Manufacturing Centre, Universiti Teknikal Malaysia Melaka, Hang Tuah Jaya, 76100 Durian Tunggal, Melaka, Malaysia

<sup>4</sup>NanoMalaysia Berhad, A-2-3, Level 2, 157 Hampshire Place Office No. 1, Jalan Mayang Sari, 50450 Kuala Lumpur.

<sup>5</sup>Institute of Science and Technology, China Railway Eryuan Engineering Group Co.Ltd, No.3 Tongjin Road, Sichuan, 610031, P.R.China

### ABSTRACT

*Graphene nanoparticles (GNP) conductive ink has become the main filler material in the formulation of conductive ink. Because of that, various efforts have been performed to obtain the influencing parameters that can affect the GNP conductive ink electrical conductivity. Based on that, this study was performed to investigate the effect of temperature, ink thickness, and shape on the sheet resistivity of GNP conductive ink. The ink formulation used was 35 wt% of GNP as filler loading and printed to form 4 types of pattern with 3 different thicknesses by using the stencil printing method. The samples were cured at three different temperatures of 90 °C, 100 °C, and 110 °C, and sheet resistivity was measured to obtain the correlation between the samples' electrical properties with the temperature, ink thickness, and shape. The results showed that sample of zigzag pattern, with the thickness of 1 mm and cured at 90 °C produced the highest average sheet resistivity of 20.77 kΩ/sq, and a sample of sinusoidal pattern, with a thickness of 3 mm and cured at 110 °C produced the lowest average sheet resistivity of 4.01 kΩ/sq. As for the trend, the increment of ink thickness and curing temperature reduces the sheet resistivity for most of the ink patterns including straight-line, square, and sinusoidal. When the design of the pattern has more curves and bends such as the zigzag pattern, the sheet resistivity value cannot be reduced by increasing the ink thickness and curing temperature. It is because the shape of the pattern becomes the main influencing parameter in determining the ink electrical conductivity.*

**Keywords:** Graphene Nanoparticles, conductive ink, sheet resistivity, temperature, morphology analysis

### 1. INTRODUCTION

Because of the new demand for electrical circuitry especially that requires contact with human skin such as in the fields of neuroscience and automotive monitoring systems, [1,2] the utilization of non-metallic-based material has become increasingly popular in recent years. It pushes the technology of conductive ink to be rapidly evolved to meet this demand. This includes the usage of carbon-based material especially graphene that produces no corrosion effect. Besides, conductive ink technology also becomes the preferred approach in the fields of printable and flexible electronics [3]. It is because the conductive ink possesses other main prominent advantages such as compatibility and producibility [4]. But the challenge of

---

\*Corresponding Author: azli@utem.edu.my

producing conductive ink is the selection of suitable material and printing techniques for specific applications.

Conductive ink requires the use of nanoparticle materials because it needs to be printed in the form of a fine line. Currently, the most popular material used for conductive ink is silver nanoparticles because of their characteristics such as oxidation stability and high electrical conductivity. In recent years, the introduction of graphene in conductive ink technology has become increasingly attractive. It is found that graphene is a zero-gap semiconductor material and possesses comparable electrical conductivity performance as silver [5] by having large electron mobility at room temperature [6]. Furthermore, graphene has better chemical stability and mechanical properties as compared to other metallic-based materials [7]. Because of that, graphene has been chosen as the main filler material for the formulation of conductive ink in this study.

One of the other important aspects of producing conductive ink is the printing method. This study employs the use of manual stencil printing to produce ink patterns. Even though there are many popular printing techniques in the field of conductive ink such as screen printing, gravure printing, inkjet printing, and 3D printing [8,9], this method is chosen because of the capability to produce a thick film in a single pass that reduces the processing time [10]. Besides, this technique can easily be repeated on the different substrates without the need to extensively change the operating procedures [8]. It is a much simpler method as compared to the other printing approaches and can be considered more versatile.

The main characteristic to measure the performance of conductive ink is electrical conductivity. For a thin film such as conductive ink, the electrical conductivity is measured in the form of sheet resistivity [11]. This approach is also applied to this study. In addition, the addition of heat is known can alter the chemical reaction inside of the composite. Because of that, it becomes the main intention of this study to investigate the effect of temperature on sheet resistivity. Furthermore, the influence of ink patterns is also investigated. Then, qualitative analysis is also performed by using microscopy techniques to obtain the correlation between surface microstructure and sheet resistivity.

## **2. MATERIAL AND METHODS**

### **2.1 Sample Preparation**

The samples of conductive ink need to be produced before any experimental work can be done. It must be performed according to the proper procedure to ensure the samples can produce accurate data for the analysis. This procedure includes formulating the ink according to the prescribed material ratio, printing the ink on the substrate, and curing the ink at different temperatures. These steps were carried out in the correct order of sequence.

#### **2.1.1 Conductive Ink Formulation**

The conductive ink formulation consists of three main components, which are the filler, binder, and hardener. The ratio of the formulation was based on the best material composition obtained by the past researcher [12]. It was based on the study of formulating the composition by having the different percentage of filler loading starting from 10 %wt up to 35 %wt with the 5 %wt increment. The ink formulation is tabulated in Table 1 below. Then, the best formulation was selected, which was the ink formulation with 35 %wt. This study was using Graphene Nanoparticles (GNP) as the filler with a specific surface area of 500 m<sup>2</sup>/g and a molecular mass of 12.01 g/mol obtained from Sigma Aldrich. It is the main ingredient in the material





composition that makes the ink capable of conducting electricity. The other component is the binder, which is functioned to combine all the materials. It is used to transform the ink from liquid-state to become ink paste [13]. Bisphenol-A diglycidyl (DGEBA) ethers epoxy resin was used as the binder. It has an average molecular density of  $\leq 700$  g/mol, resin density of 1,168 g/ml, and viscosity value of 500 to 750 mPa.s at 25 °C. Then, the Hunstman polyetheramine D230 was used as a hardener with a concentration of 0.947 g/ml and viscosity of 9 mPa.s at 25 °C. Based on the literature, the electrical conductivity of composite can be enhanced by increasing the filler content [8]. The enhancement of electrical conductivity performance is relying on the formation of the conductive path in the composition. But the process of increasing the filler loading in the composition will increase the cost of the samples because these conductive fillers are the most expansive as compared to other material components. Because of that, it is necessary to obtain the optimum amount of filler loading that can produce comparable performance. This was done by a previous researcher by obtaining the least amount GNP filler requires to have similar performance [14]. Then, the centrifugal mixer, which is called a Thinky mixer was used to mix the materials according to their individual weight at the speed of 2,000 rpm for 3 minutes.

**Table 1** Formulation of GNP conductive ink

	Filler		Binder		Hardener (g)	Total (g)
	(wt.%)	(g)	(wt.%)	(g)		
1	10	0.2	90	1.8	0.54	2.54
2	15	0.3	85	1.7	0.51	2.51
3	20	0.4	80	1.6	0.48	2.48
4	25	0.5	75	1.5	0.45	2.45
5	30	0.6	70	1.4	0.42	2.42
6	35	0.7	65	1.3	0.39	2.39

### 2.1.2 Printing Method

Manual stencil printing was used to produce the patterns of the GNP ink. A prefabricated stencil was prepared with the detailed geometrical pattern as shown in Figure 1. It consists of four different patterns, which are straight-line, sinusoidal, square, and zigzag to mimic the widely use pattern in printing electrical circuitry in the electronics industry. The ink paste was deposited on the substrate by using this stencil. It is because this technique is suitable to print ink patterns on various types of ink especially with low resistivity [15]. It is also considered a simple and fast way of producing multiple patterns at the same time. For this study, Thermoplastic polyurethane (TPU) was used as the substrate because it possesses the stretchability characteristic that is required for this study. TPU can withstand a high-temperature process and recover the rubber-like property during solidification [16]. Each of the patterns was printed in 3 different ink thicknesses, which are 1 mm, 2 mm, and 3mm.

Patterns	Shape
Straight-line	
Zigzag	
Square	
Sinusoidal	

**Figure 1.** Conductive ink test patterns.

### 2.1.3 Curing Process

The variability of the testing procedure in this study was performed by this curing process. It can be described as the post-treatment of the ink samples by using heat. The purpose of the curing process is to anneal the composition by removing the excess solvent and encouraging the chemical reaction to occur to form the conductive network paths. It can also enhance the adhesion of GNP inks to the TPU substrate [17]. For this study, universal oven UF55 was used to cure the samples at various temperatures. Three different temperatures were used for the curing process, which are 90, 100, and 110 °C for 30 minutes. After underwent the curing process in the oven, then, the samples were dried at room temperature.

## 2.2 Sample Characterization

In this study, the testing procedures were performed by characterizing the samples to determine the related parameters of the electrical and microstructure properties. These procedures were carried out for all the samples with the variability of pattern, thickness and curing temperature. Firstly, the precise locations of the measurement points on the sample were determined. These measurement points are shown in Figure 2 below. The purpose is to ensure that the consistent data can be obtained when analyzing them. Furthermore, the locations of the measurement points were chosen as to have the balanced distribution of data collection from the samples.

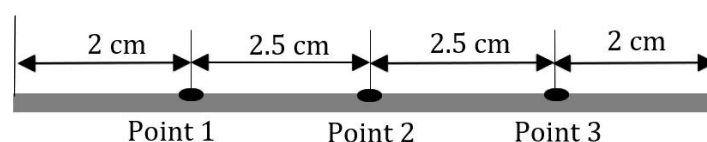


**Figure 2.** The location of measurement points on the sample.

### 2.2.1. Electrical Properties

For the electrical properties, the investigated parameter is sheet resistivity. It is measured at all the samples of different thicknesses, patterns, and curing temperatures. For the thin layer of

conductive ink, sheet resistivity is more suitable to be examined as compared to bulk resistivity [11]. The equipment used for the measurement was the JANDEL In-Lane Four-point Probe with 1 mm distance between each probe by referring to ASTM F390 standard [10].

### **2.2.2. Microstructure Properties**

The microstructure properties were investigated by obtaining the microstructure images of the GNP ink layer surface using the microscopy technique. These images were obtained at three different resolutions, which are 5x, 10x, and 20x. for all the samples of different thicknesses, patterns, and curing temperatures. The qualitative analysis was performed by observing the particle's size, shape, profile, and structure of the ink layer surface. The addition of heat to the composition provides external energy for molecular movement. It can alter the atomic and molecular arrangement of the compound [6].

## **3. RESULTS AND DISCUSSION**

### **3.1. Analysis of Sheet Resistivity**

The analysis about sheet resistivity was performed to determine the electrical characteristics of GNP conductive ink. The electrical conductivity performance of the material can be determined by obtaining the sheet resistivity values, especially for thin layer material. It is inversely proportional to electrical conductivity. In this study, the sheet resistivity values were obtained for samples of 4 different patterns with 3 different thicknesses with the effect of 3 different temperatures. Then, the direct correlation between the ink pattern dan temperature can be achieved.

#### **3.1.1. Sheet Resistivity for Temperature of 90 °C**

The data of sheet resistivity for the samples with different thicknesses and patterns cured at 90°C are shown in Figure 3 below. All the samples show almost the same trend for all different patterns. All the patterns show that the samples with a thickness of 1 mm have the highest sheet resistivity as compared to the other thickness for all the patterns. With the increment of thickness, it reduces the sheet resistivity.

For the straight-line pattern, the samples with a thickness of 1 mm produce average sheet resistivity of 14.54 kΩ/sq. Then, the samples with the thickness of 2 mm and 3mm produce the average sheet resistivity of 12.98 kΩ/sq and 10.25 kΩ/sq. The data for this pattern also has the highest average standard error, with the values of 2.37 for 1 mm of thickness, 1.73 for 2 mm of thickness, and 2.13 for 3 mm of thickness.

For the zigzag pattern, the highest average sheet resistivity is for the thickness of 1 mm with the value of 20.77 kΩ/sq, which is also the highest value for the samples cured at 90 °C. The samples of 2 mm and 3 mm thicknesses produce the average of 11.03 kΩ/sq and 10.90 kΩ/sq of sheet resistivity values. The data for this pattern also has the least standard error for the data distribution, which is based on the standard deviation except for the 3 mm thickness. The data for 3 mm of thickness show proximity with the data of 2 mm because of the error.

The samples of sinusoidal pattern produce the second-highest sheet resistivity values. The samples with 1 mm thickness produce an average of 19.59 kΩ/sq and follow by 2 mm and 3 mm thicknesses with the average values of 13.61 kΩ/sq and 10.82 kΩ/sq. For the square pattern, the samples of 1 mm of thickness produce 14.96 kΩ/sq. It reduces to 13.11 kΩ/sq for 2 mm of thickness and 9.78 kΩ/sq for 3 mm of thickness. The increase of thickness reduces the sheet resistivity.

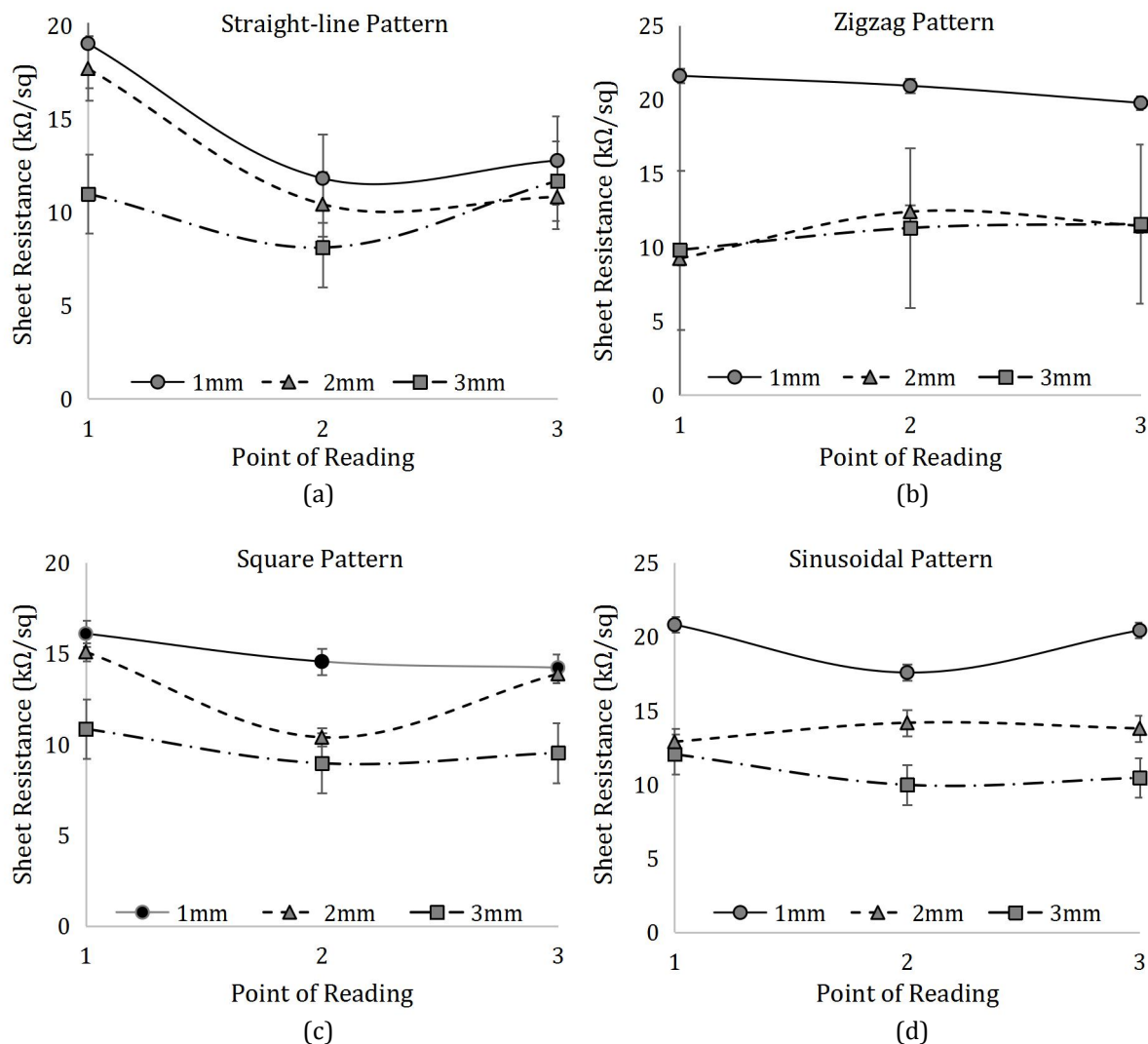


**Figure 3.** Sheet resistivity for samples of different thicknesses cured at 90 °C for (a) straight-line, (b) zigzag, (c) square and (d) sinusoidal patterns.

### 3.1.2 Sheet Resistivity for Temperature of 100 °C

For the samples cured at a temperature of 100 °C, the data is illustrated in Figure 4 below. The zigzag pattern still shows the highest average sheet resistivity values. The 1 mm of thickness produces 19.23  $k\Omega/sq$ , follows by 2 mm of thickness with 17.06  $k\Omega/sq$  and 3 mm of thickness with the value of 12.77  $k\Omega/sq$ . This pattern also has the lowest average of standard error in the range between 0.32 to 0.83.

The second-highest average of sheet resistivity is for the square pattern. This pattern produces the average values of 16.14  $k\Omega/sq$ , 11.71  $k\Omega/sq$ , and 7.90  $k\Omega/sq$  for thicknesses of 1 mm, 2 mm, and 3 mm, respectively. Then, the sinusoidal pattern produces 15.20  $k\Omega/sq$  for 1 mm of thickness, 11.61  $k\Omega/sq$  for 2 mm of thickness, and 7.91  $k\Omega/sq$  for 3 mm of thickness. This pattern has the lowest average of standard error for the data. The straight-line pattern produces the least average sheet resistivity for the samples cured at 100 °C. The samples of 1 mm of thickness produce an average value of 11.88  $k\Omega/sq$  and follow by 2 mm and 3 mm of thicknesses with the average values of 8.80  $k\Omega/sq$  and 6.38  $k\Omega/sq$ . But, this pattern has the highest range of data standard error. In general, it still shows that the increment of thickness reduces the sheet resistivity for all the patterns.

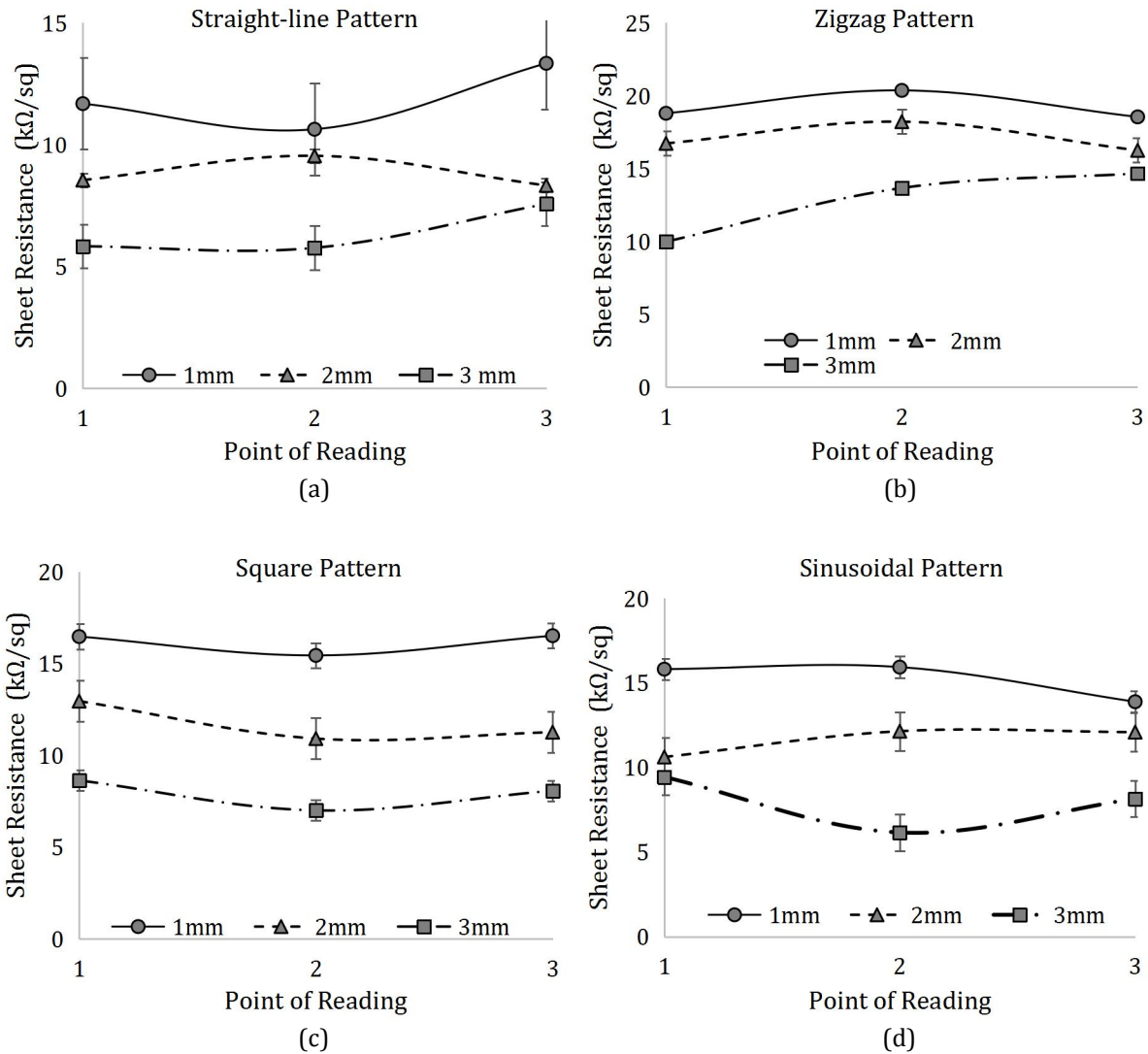


**Figure 4.** Sheet resistivity for samples of different thicknesses cured at 100 °C for (a) straight-line, (b) zigzag, (c) square and (d) sinusoidal patterns.

### 3.1.3. Sheet Resistivity for Temperature of 110 °C

Figure 5 below shows the data for the samples cure at 110 °C. The samples cured at this temperature show the same trend as the samples cured at 90 °C and 100 °C. The increase of sample thickness reduces the average of sheet resistivity values. The lowest recorded average sheet resistivity is for a straight-line pattern with the values of 9.07 kΩ/sq for 1 mm of thickness, 5.87 kΩ/sq for 2 mm of thickness, and 4.76 for 3 mm of thickness. The value for 3 mm of a thickness of straight-line pattern is also the lowest measured average sheet resistivity recorded among the entire samples in this study.

The highest average sheet resistivity values recorded for the samples cure at 110 °C are for the zigzag pattern. The thickness of 1 mm produces the average value of 18.13 kΩ/sq. The thicknesses of 2 mm and 3 mm produce 14.09 kΩ/sq and 8.82 kΩ/sq. All the bends and corners of the pattern produce a greater effect at the boundary conditions, which causes the boundary to become thicker and loosen. These occurrences were also mentioned in previous findings [21,22]. Meanwhile, for the square pattern, the thicknesses of 1 mm, 2 mm, and 3 mm produce 12.23 kΩ/sq, 8.68 kΩ/sq, and 6.11 kΩ/sq, respectively. For the sinusoidal pattern, the average

sheet resistivity values are 12.55 kΩ/sq for 1 mm of thickness, 8.74 kΩ/sq for 2 mm of thickness, and 5.35 kΩ/sq for 3 mm of thickness.

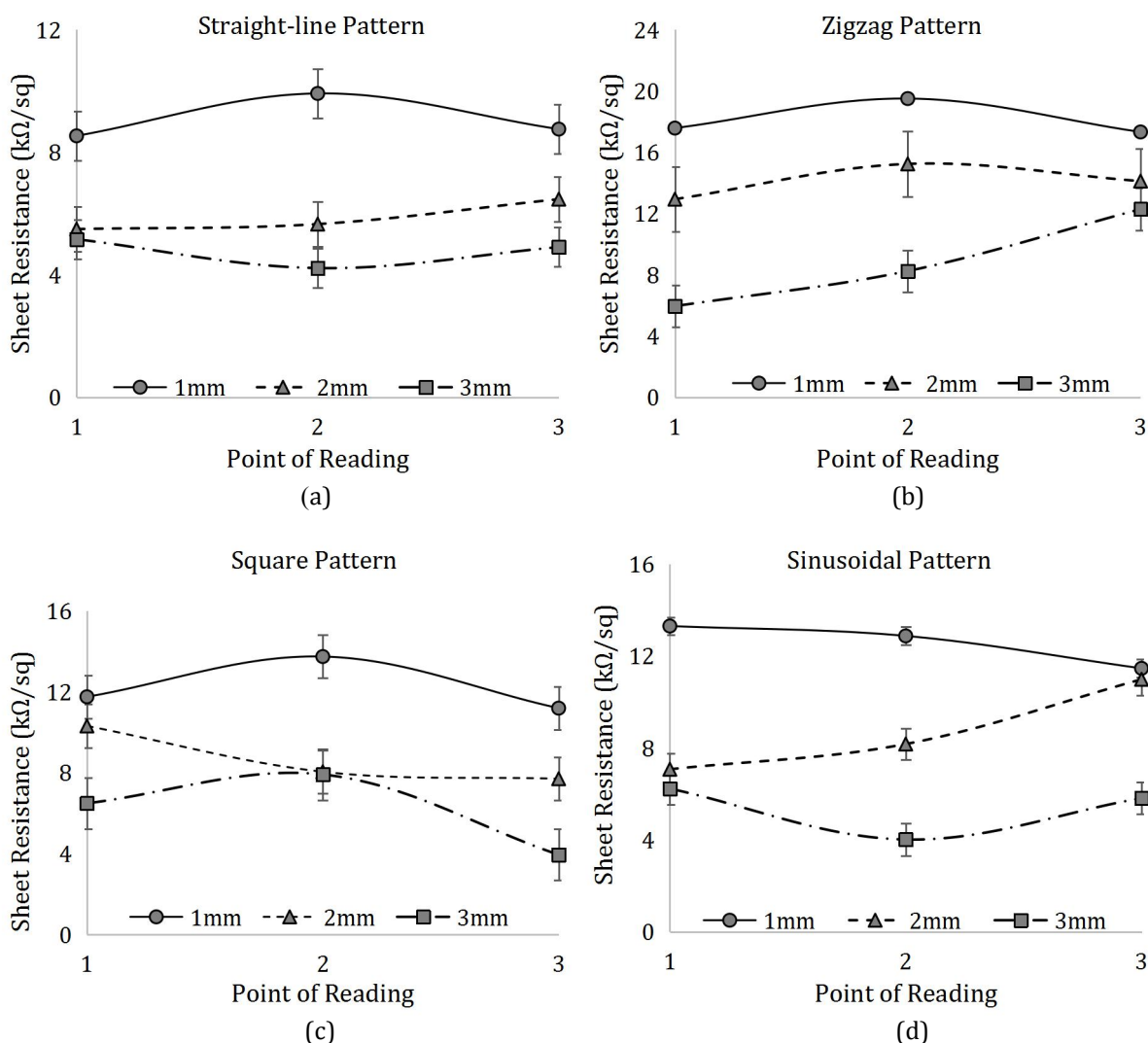


**Figure 5.** Sheet resistivity for samples of different thicknesses cured at 110 °C for (a) straight-line, (b) zigzag, (c) square and (d) sinusoidal patterns.

### 3.2. Correlation between Sheet Resistivity and Temperature

The correlation between sheet resistivity and temperature for samples with different thicknesses and patterns is shown in Figure 6 below. For the patterns of straight-line and sinusoidal, they show a direct correlation between sheet resistivity and temperature. The increase of temperature reduces the sheet resistivity for all the thicknesses. The thickness of 1 mm has the highest sheet resistivity, and the increment of thickness reduces the sheet resistivity. The straight-line pattern shows the lower range of sheet resistivity among all thicknesses and temperature, which is in between 6.56 kΩ/sq to 14.54 kΩ/sq. The sinusoidal pattern produces a higher magnitude of sheet resistivity in between 8.88 kΩ/sq to 19.59 kΩ/sq.

The square pattern also shows the same correlation between sheet resistivity and temperature except for the thickness of 1 mm. The sheet resistivity for the sample cured at 100 °C is higher than at 90°C. Other than that, one measurement point, all the other data, show the same correlation. Among all the patterns, the only zigzag pattern shows the different trend. For the



thicknesses of 2 mm and 3 mm, they do not show any direct correlation between sheet resistivity and temperature especially for the sample with the thickness of 2 mm. With the increase of temperature from 90 °C to 100 °C, it shows a significant increase in sheet resistivity from 11.03 kΩ/sq to 17.06 kΩ/sq. Then, the value decreases to become 14.10 kΩ/sq at the temperature of 110 °C. With the increase of pattern thickness, the shape of the pattern produces greater influence as opposed to the increase of conductive path cross-sectional area. It confirms the findings in the literature [18].

The overall correlation between sheet resistivity and temperature for different ink patterns can be obtained as shown in Figure 7 below. It is illustrated by using the average values of sheet resistivity of different thicknesses for every pattern. The straight-line and sinusoidal patterns clearly show the same trend, which is the direct correlation between these two parameters. The increase of temperature directly decreases the sheet resistivity at different magnitudes. The reduction for the straight-line pattern is from 12.59 kΩ/sq to 6.56 kΩ/sq and for the sinusoidal pattern is from 14.67 kΩ/sq to 8.88 kΩ/sq. The square pattern still shows the reduction of sheet resistivity with the increase of temperature, but it is not in direct proportion. The sheet resistivity values are decreasing from 12.26 kΩ/sq to 5.52 kΩ/sq.

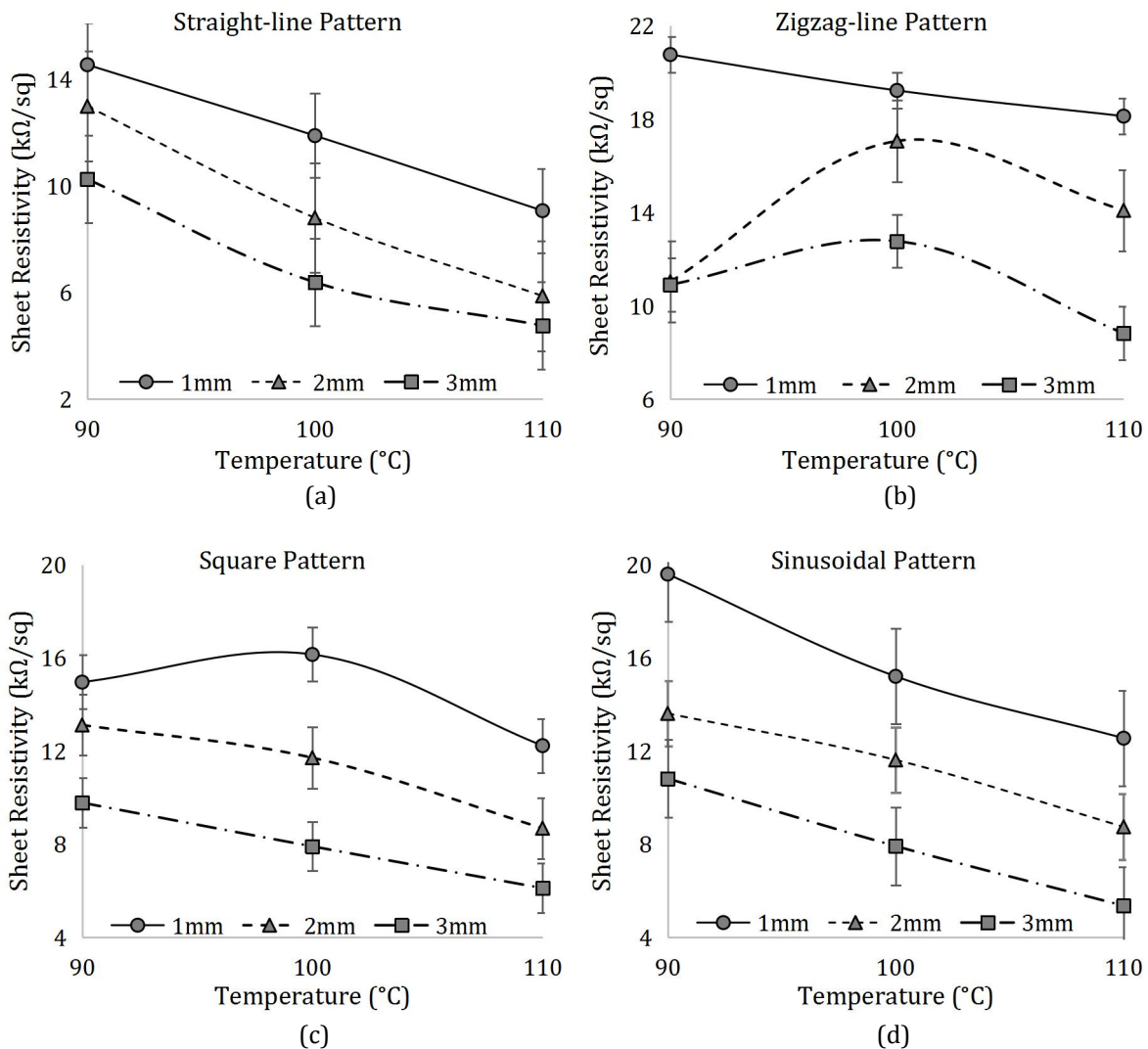


**Figure 6.** Sheet resistivity for samples of different thicknesses with the increase of temperature for (a) straight-line, (b) zigzag, (c) square, and (d) sinusoidal patterns.

Among all the patterns, only the zigzag pattern shows a different trend. The increase of temperature from 90 °C to 100 °C increases the sheet resistivity values significantly from 14.23 kΩ/sq to 16.35 kΩ/sq. Then, the value decreases to become 13.68 kΩ/sq at the temperature of 110 °C. This specific occurrence was explained by past research [21]. In terms of the magnitude of average sheet resistivity values, the straight-line pattern shows the lowest values. It follows by sinusoidal, square, and finally the zigzag pattern.

In general, the increase of the temperature reduces the sheet resistivity by removing the excess solvent and encouraging the chemical reaction to occur to form the conductive network paths. This condition was also explained by previous research [17]. It improves the conductivity of the GNP conductive ink.

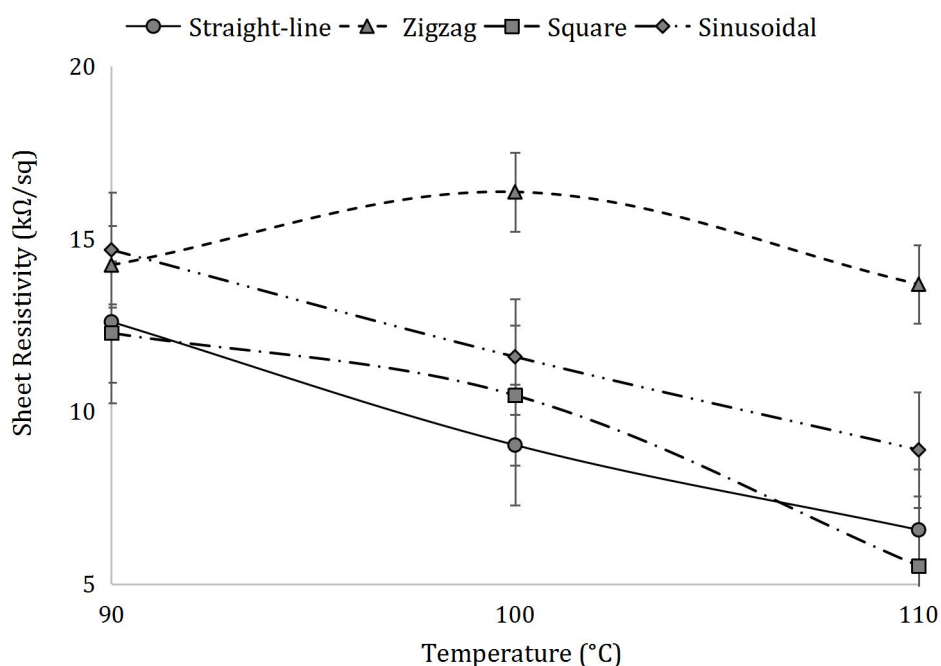


**Figure 7.** Average sheet resistivity vs temperature for samples of different patterns.

### 3.3. Analysis of Morphology

The morphological analysis was performed based on the microscopy images, which were captured for all the samples of different thicknesses, patterns, and curing temperatures. For each sample, the microscopy images were captured at three different locations on the sample with three different resolutions. But for the purpose of comparison, only the microscopy images for the samples that produce the best and worst sheet resistivity values are going to be discussed. These images were captured at three different locations with the highest magnification of 20x.

Figure 8 below shows the microscopy images for the samples of zigzag pattern, with the thickness of 1 mm and cured at 90 °C. It is the worst recorded sheet resistivity among all the samples in this study with an average value of 20.77 kΩ/sq. The ink layer surface shows the presence of bumps as labeled by continuous circles in the figure that reduces the homogeneity of the composition. Because of that, it reduces the density of conductive particles inside the material. This condition is also explained in the literature [20]. This causes the high value of sheet resistivity of the sample. Furthermore, the ink layer surface also indicates the defect such as creases as labeled by dashed circles in the figure. The occurrence of this defect had been explained by previous research [24, 27]. It is caused by the mismatch in crystallographic

orientation or alignment of graphene lattice in various grains. Because of that, it increases the particle gap that restricts the movement of electrons.

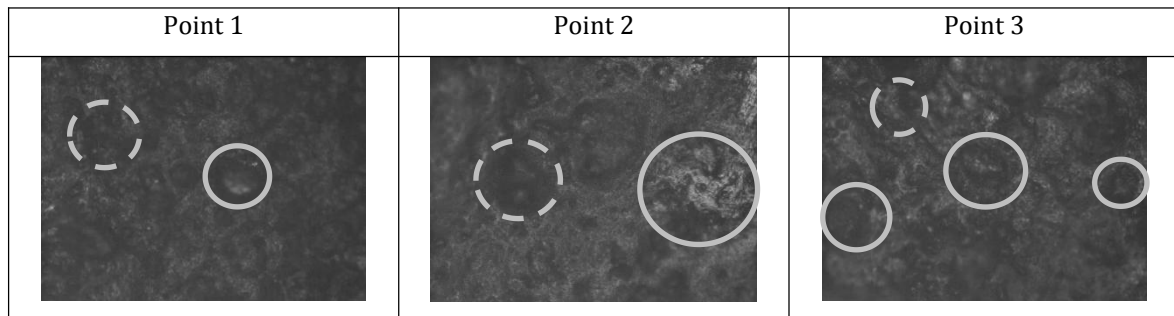


**Figure 8.** Microscopy images for samples of zigzag pattern, thickness of 1 mm and cured at 90 °C.

Figure 9 below shows the microscopy images for the samples of sinusoidal pattern, with the thickness of 3 mm and cured at 110 °C. It is the best-recorded sheet resistivity among all the samples in this study with an average value of 4.01 kΩ/sq. The microscopy images illustrate the most homogenous composition with the well-distributed arrangement of particles. It produces less gap between the conductive particles that allows the movement of electrons to flow between the particles. Thus, it increases the electrical conductivity of the composition as mentioned in [5]. The well-distributed particles are also portrayed with less existence of ridges and creases. This indicates a good dispersion of GNP in the composition that forms proper conductive filler particle arrangement. It facilitates the electron tunneling effect, which increases the electrical conductivity behavior of the ink. This occurrence is also explained in the findings of previous research. [6][23]

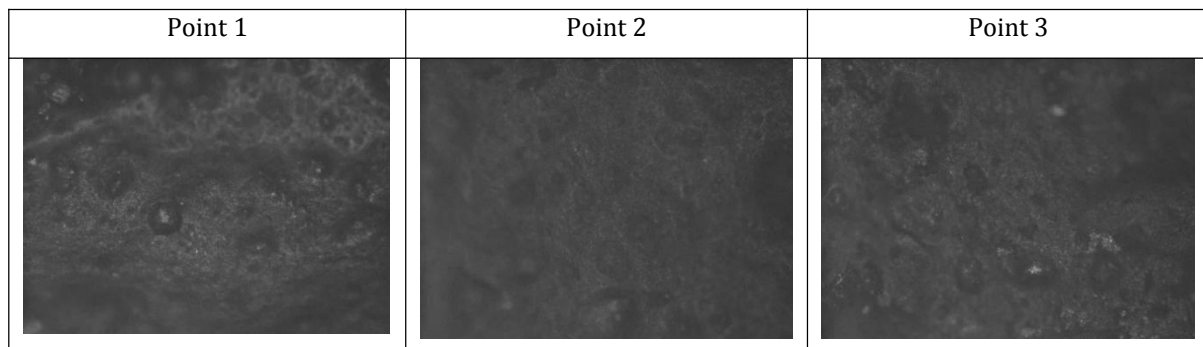


**Figure 9.** Microscopy images for sample of sinusoidal pattern, thickness of 3 mm and cured at 110 °C.

#### 4. CONCLUSION

This study was performed to investigate the effect of temperature, thickness, and shape on sheet resistivity for GNP conductive ink. The ink formulation used was 35 wt% of GNP as filler loading and printed to form 4 types of pattern with 3 different thicknesses by using the stencil printing method. The samples were cured at three different temperatures of 90 °C, 100 °C, and 110 °C, and sheet resistivity was measured to obtain the correlation between the samples' electrical properties with the temperature, ink thickness, and shape. The results showed that sample of zigzag pattern, with the thickness of 1 mm and cured at 90 °C produced the highest sheet resistivity of 20.77 kΩ/sq, and a sample of sinusoidal pattern, with the thickness of 3 mm and cured at 110 °C produced the lowest sheet resistivity of 4.01 kΩ/sq. As for the trend, the increment of ink thickness and curing temperature reduces the sheet resistivity for most of the ink patterns including straight-line, square, and sinusoidal. When the design of the pattern has

more curves and bends such as the zigzag pattern, the sheet resistivity value cannot be reduced by increasing the ink thickness and curing temperature. It is because the shape of the pattern becomes the main influencing parameter in determining the ink electrical conductivity.

## ACKNOWLEDGEMENTS

Special thanks to the Advanced Academia-Industry Collaboration Laboratory (AiCL) and Fakulti Kejuruteraan Mekanikal (FKM), Universiti Teknikal Malaysia Melaka (UTeM) for providing the laboratory facilities.

## REFERENCES

- [1] Y. Chen *et al.*, "How is flexible electronics advancing neuroscience research?," *Biomaterials*, vol. **268**, no. December 2020, (2021) pp.120559.
- [2] A. K. Ab Wahid *et al.*, "Driving monitoring system application with stretchable conductive inks: A review," *Int. J. Nanoelectron. Mater.*, vol. **13**, no. Special Issue ISSTE 2019, (2020) pp.327–346.
- [3] Y. Liu, W. Zhang, H. Yu, Z. Jing, Z. Song, and S. Wang, "A concise and antioxidative method to prepare copper conductive inks in a two-phase water/xylene system for printed electronics," *Chem. Phys. Lett.*, vol. **708**, (2018) pp.28–31.
- [4] W. Li *et al.*, "The rise of conductive copper inks: challenges and perspectives," *Appl. Mater. Today*, vol. **18**, (2020) pp.100451.
- [5] M. Mokhlis *et al.*, "Electrical Performances of Graphene Materials with Different Filler Loading for Future Super Conductor," *Def. S T Tech. Bull.*, vol. **12**, no. 2, pp. 193–201, 2019.
- [6] S. K. Kulkarni, *Nanotechnology - Principles and Practices 3rd ed (Springer, CP, 2015).pdf*. 2014.
- [7] Z. Zhang, J. Sun, C. Lai, Q. Wang, and C. Hu, "High-yield ball-milling synthesis of extremely concentrated and highly conductive graphene nanoplatelet inks for rapid surface coating of diverse substrates," *Carbon N. Y.*, vol. **120**, (2017) pp.411–418.
- [8] T. S. Tran, N. K. Dutta, and N. R. Choudhury, "Graphene inks for printed flexible electronics: Graphene dispersions, ink formulations, printing techniques and applications," *Adv. Colloid Interface Sci.*, vol. **261**, (2018) pp.41–61.
- [9] Č. Žlebič *et al.*, "Electrical properties of inkjet printed graphene patterns on PET-based substrate," *Proc. Int. Spring Semin. Electron. Technol.*, vol. **2015-Septe**, (2015) pp.414–417.
- [10] H. Saad, M. A. Salim, N. Azmmi Masripan, A. M. Saad, and F. Dai, "Nanoscale graphene nanoparticles conductive ink mechanical performance based on nanoindentation analysis," *Int. J. Nanoelectron. Mater.*, vol. **13**, no. Special Issue ISSTE 2019, (2020) pp.439–448.
- [11] S. A. Peng *et al.*, "The sheet resistance of graphene under contact and its effect on the derived specific contact resistivity," *Carbon N. Y.*, vol. **82**, no. C, (2015) pp.500–505.
- [12] M. Mokhlis, "A Study on Electrical and Mechanical Properties of Hybrid Ink Nanocomposite," Universiti Teknikal Malaysia Melaka, 2019.
- [13] N. Ismail *et al.*, "The behaviour of graphene nanoplatelets thin film for high cyclic fatigue," *Int. J. Nanoelectron. Mater.*, vol. **13**, no. Special Issue ISSTE 2019, (2020) pp.305–314.
- [14] M. Mokhlis *et al.*, "Nanoindentation of graphene reinforced epoxy resin as a conductive ink for microelectronic packaging application," *Int. J. Nanoelectron. Mater.*, vol. **13**, no. Special Issue ISSTE 2019, (2020) pp.407–418.
- [15] L. Liu, Z. Shen, X. Zhang, and H. Ma, "Highly conductive graphene/carbon black screen printing inks for flexible electronics," *J. Colloid Interface Sci.*, vol. **582**, (2021) pp.12–21.
- [16] N. Ismail *et al.*, "Resistivity characterization for carbon based conductive nanocomposite

- on polyethylene terephthalate and thermoplastic polyurethane substrates," *Int. J. Nanoelectron. Mater.*, vol. **13**, no. Special Issue ISSTE 2019, (2020) pp.315–326.
- [17] Y. Z. N. Htwe, M. K. Abdullah, and M. Mariatti, "Optimization of graphene conductive ink using solvent exchange techniques for flexible electronics applications," *Synth. Met.*, vol. **274**, no. December 2020, (2021) pp.116719.
- [18] J. Y. Park, W. J. Lee, B. S. Kwon, S. Y. Nam, and S. H. Choa, "Highly stretchable and conductive conductors based on Ag flakes and polyester composites," *Microelectron. Eng.*, vol. **199**, no. January, (2018) pp.16–23.
- [19] W. Zhang, M. Li, L. Gao, and X. Ban, "Surface characterization and electrical properties of spin-coated graphene conductive film," *16th Int. Conf. Electron. Packag. Technol. ICEPT 2015*, (2015) pp.56–59.
- [20] A. Çelik *et al.*, *Carbon Nanotechnology Recent Developments in Chemistry, Physics, Material Science and Device Applications*, vol. **1**, no. 1, (2006).
- [21] H. A. D. Nguyen, N. Hoang, K. H. Shin, and S. Lee, "Improvement of surface roughness and conductivity by calendering process for printed electronics," *URAI 2011 - 2011 8th Int. Conf. Ubiquitous Robot. Ambient Intell.*, no. November, (2011) pp.685–687.
- [22] A. J. M. Giesbers *et al.*, "Defects, a challenge for graphene in flexible electronics," *Solid State Commun.*, vol. **229**, (2016) pp.49–52.
- [23] T. Khan, M. S. Irfan, M. Ali, Y. Dong, S. Ramakrisna, and R. Umer, "Insights to low electrical percolation thresholds of carbon-based polypropylene nanocomposites," *Sci. Total Environ.*, (2019) pp.135907.

